

Supplementary material and methods:

Cell lines

The details of the EBNA2 coding sequence carrying B95-8 and EBNA2 negative P3HR1 strain infected BLs are in Supplementary Table 1. All cells were cultured in RPMI-1640 medium, supplemented with 10% fetal bovine serum (FBS), 100 U/mL penicillin, 100µg/mL streptomycin, and L-glutamine. Cell lines were maintained at 37°C in an incubator in a humidified atmosphere of 5% CO₂.

Immunoblotting

The PVDF membranes were stained with Ponceau Red to confirm the success of the transfer, then washed with PBS-Tween 0,1% (PBS-T) and incubated for 1 hour in a blocking buffer, composed of 5% non-fat dried milk in PBS-T. EBNA2 expression was verified by using a mouse monoclonal antibody, PE2 (Novus, Bio-Techne) at 1:250 dilution in milk 5% PBS-T. The expression of c-MYC was detected by a rabbit monoclonal antibody c-Myc (D84C12) (Cell Signaling Technology) and β-actin (Santa Cruz Biotechnology) was used as a loading control. As secondary antibodies, HRP conjugated mouse (Millipore-Sigma) or goat anti-rabbit (ADVASTA) abs were used. The proteins were detected using Western Bright ECL HRP chemiluminescent substrate kit and the images acquired by an automatic developer. Each immunoblot was repeated at least three times. Bcl-2 expression was verified by using a rabbit monoclonal antibody, (D55G8, Cell Signaling) at 1:250 dilution in milk 5% PBS-T. β-actin (Santa Cruz Biotechnology) was used at 1:5000 in BSA 5% as a loading control.

Densitometry analysis of immunoblots

Densitometry analysis was performed with Image J 1.53t. Quantification of protein bands, corresponding to EBNA2, c-Myc, and BCL2 expression and the loading control β-actin, was measured by inverting the pixel density of each protein band as 255-x (x is the “Grey mean value” recorded by ImageJ). The inverted background was then subtracted from the inverted band value. Finally, the relative quantification of each protein band was calculated as a ratio: EBNA2/ β-actin, c-Myc/ β-actin, and BCL2/ β-actin.

Prediction of miR-24 as a potential ICOSL targeting miRNA

To better understand the molecular mechanisms of ICOSL downregulation by EBNA2, several previous observations were helpful that led us to focus on miR-24. Cameron et al (2008) had shown that Lat III expressing BLs express higher miR-24. Our published data also indicated that EBNA2 transfected U2932 DLBCL cells have higher miR-24 (Rosato et al, 2012).³⁰ A bioinformatic analysis had suggested regulation of ICOSL expression by miR-24 (Veksler-Lublinsky et al).⁴⁸ Similarly, a couple of miRNA-mRNA prediction algorithms like TargetScan and miRWalk identified ICOSL as a potential target of miR-24.

TargetScan 8.0 predicts biological targets of miRNAs by searching for the presence of conserved 8mer, 7mer, and 6mer sites that match the seed region of each miRNA (Lewis et al., 2005). As seen in the table below the metrics used for the strength of predictions are:

A: The site type strongly influences the efficacy of repression. The most effective in order of decreasing preferential conservation and efficacy sites are:

-8mer, (Watson–Crick match to miRNA positions 2–8 with an A opposite position 1

-7mer-m8, (position 2–8 match) and

-7mer-A1 sites, (position 2–7 match with an A opposite position 1) (Lewis et al., 2005).

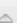

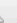





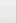
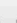

As seen in the table below, in the case of miR-24-ICOSL pairing, the type of sites are the most effective and the number of sites (four) may impart additional repression.

B: The context⁺⁺ score (CS) of miRNA targeting efficacy for a specific site is the sum of 14 different features of the miRNA, miRNA site, or mRNA—including the mRNA sequence around the site—to predict which sites within mRNAs are most effectively targeted by miRNAs (Agarwal et al., 2015).

The context score thus is the sum of these features and a negative score is associated with a more favorable site. In addition, a high context score percentile (between 50 and 100) shows that a specific site is more favorable than most other sites of this miRNA. Indeed, as seen in the table below, the miR-24 and ICOSL interaction context score and the context score percentile indicate this interaction as very likely.

	Predicted consequential pairing of target region (top) and miRNA (bottom)	Site type	Context++ score	Context++ score percentile	Weighted context++ score	Conserved branch length	P _{CT}
Position 669-675 of ICOSLG 3' UTR hsa-miR-24-3p	5' . . . GUUCCGGUGAAAAGUUGAGCCAC . . . 3' GACAAGGACGACUUG--ACUCGGU	7mer-A1	-0.09	77	-0.09	0.017	< 0.1
Position 1493-1499 of ICOSLG 3' UTR hsa-miR-24-3p	5' . . . AAAAAAGUCCUACCUAGACCU . . . 3' GACAAGGACGACUUGACUCGGU	7mer-m8	-0.19	91	-0.19	0	< 0.1
Position 3725-3732 of ICOSLG 3' UTR hsa-miR-24-3p	5' . . . CCGCCCAUCCUCAUC--CUGAGCCA . . . 3' GACAAGGACGACUUGACUCGGU	8mer	-0.03	57	0.00	0.042	< 0.1
Position 4344-4350 of ICOSLG 3' UTR hsa-miR-24-3p	5' . . . UUAUUUUUUUUUUUUUGAGCCAG . . . 3' GACAAGGACGACUUGACUCGGU	7mer-A1	-0.07	72	-0.01	0.229	< 0.1

As for the miRwalk prediction, the score is calculated from a random-forest based approach by executing TarPmiR algorithm for miRNA target site prediction. Based on the training data, it shows the probability that this interaction "works". As seen in the table below, the score=1 regarding miR-24 interaction with its target ICOSL at two CDS sites indicates that there is a high probability that this interaction will happen.

Interactions									
Mirna 	Refseqid 	Genesymbol 	Duplex 	Score 	Position 	Binding Site 	Au 	Me 	N Pairings 
hsa-miR-17-5p	NM_001283050	ICOSLG	details	0.85	CDS	969,1008	0.43	-11.681	16
hsa-miR-17-3p	NM_001283050	ICOSLG	details	0.92	CDS	969,1006	0.41	-6.236	19
hsa-miR-19a-5p	NM_001283050	ICOSLG	details	0.85	CDS	210,231	0.41	-9.061	17
hsa-miR-19b-1-5p	NM_001283050	ICOSLG	details	0.92	CDS	946,970	0.35	-15.567	17
hsa-miR-21-3p	NM_001283050	ICOSLG	details	0.85	CDS	933,956	0.37	-8.304	18
hsa-miR-22-5p	NM_001283050	ICOSLG	details	1.00	CDS	211,253	0.5	-7.782	15
hsa-miR-23a-5p	NM_001283050	ICOSLG	details	1.00	CDS	320,343	0.44	-5.481	17
hsa-miR-24-1-5p	NM_001283050	ICOSLG	details	0.92	CDS	195,218	0.41	-8.005	16
 hsa-miR-24-3p	NM_001283050	ICOSLG	details	1.00	CDS	635,676	0.48	-7.238	14
hsa-miR-24-3p	NM_001283050	ICOSLG	details	1.00	CDS	457,480	0.46	-4.994	18

Quantitative real time PCR

RNA was extracted from 1×10^6 cells. One μ l of each cDNA sample was subjected to qPCR to amplify the mature miR-24 (also known as miR-24-3p) and the housekeeping RNAU6 (TaqMan® Assays, Thermo Fisher Sc.). All the q-PCRs were performed in an Applied Biosystems\StepOne Software v2.2.2 QPCR machine. The fold change of each transcript was calculated by the $2^{-\Delta\Delta C_t}$ formula.

Flow cytometry analysis

CD4⁺ and CD8⁺ T cells were stained respectively with APC mouse anti-human and Pacific Blue mouse anti-human (BD Pharmingen) antibodies. Interferon- γ was detected with PE.Cy7 mouse anti-human IFN- γ . The staining was performed using the BD cytofix/cytoperm plus

fixation/permeabilization kit, containing the Golgi plug protein transport inhibitor, brefeldin (BD Biosciences).

Digital droplet PCR

Forty ng RNA was used for cDNA synthesis. The PCR mixture was loaded in a disposable droplet generator to create oil-emulsion droplets and transferred to a 96-well PCR plate, sealed, and quantified at the endpoint in a QX200 Droplet Reader System using QuantaSoft software (Bio-Rad Laboratories, Hercules, CA, USA). The fraction of positive droplets was quantified assuming a Poisson distribution. The samples were run in triplicates, and the concentration results were expressed as the number of copies of each transcript/ μL sample.

Mixed lymphocyte reactions

After separation, PBMCs were seeded in 24-well non-tissue culture-treated plates (Falcon, Fisher, Pittsburgh, PA, USA), previously coated with anti-CD3 and anti-CD28 (Pharmingen, San Diego, CA, USA) at the concentration of $1\ \mu\text{g}/\text{mL}$ in PBS at $0.4\ \text{mL}/\text{well}$ overnight at $4^\circ\ \text{C}$. The next day, after washing the plates in $1\ \text{ml}$ PBS, PBMCs were added to the CD3/CD28 coated wells at a density of one million cells/well and cultivated for 72 hours in order to activate the CD4⁺ and CD8⁺ T cell population. One day before seeding, 1×10^5 stimulators U2932 MPA vector and U2932 EBNA2 cl-1 cells were transiently transfected with $40\ \text{nM}$ miR-24 inhibitor and the corresponding negative control. The stimulators were then exposed to a sub-lethal dosage of 5Gy for two minutes and subsequently placed in co-culture with activated 1×10^6 PBMCs for 48 hours.

Apoptosis and cell proliferation assays

The detection of the percentage of early apoptotic (only Annexin V), late apoptotic (both Annexin V/7-AAD) and necrotic cells (only 7AAD) was done 48h post-transfection, by using CytoFLEX Flow Cytometer (Beckman coulter Life Sciences) and analyzed with CytExpert software.

As for the cellular proliferation assays, 2×10^5 cells/ml were seeded and counted daily. Trypan blue exclusion assay was performed to estimate the number of cells/ml at 24, 48, 72 and 96 hours, after transfecting U2932 vector or EBNA2 transfectants with control inhibitor or anti-miR-24. Statistical significance was calculated with ordinary one-way ANOVA Tukey's multiple comparisons test.

DLBCL cohort

We interrogated our archives both at Sapienza and Siena Universities for DLBCL cases diagnosed at our centers between 2018 and 2023. A total of 1113 DLBCLs were found. Twenty-two cases representing different DLBCL types were selected for further studies. The cohort is enriched in EBNA2 positive cases. Eight out of nine EBNA2⁺ cases were included in the study. One EBNA2 positive case from the Siena cohort was unavailable.

Immunohistochemistry

For EBNA2 IHC, sections were deparaffinized (BOND DeWax Solution, Leica Biosystems) and rehydrated with graded ethanol to distilled water. Antigen retrieval was performed in BOND Epitope Retrieval Solution 2 (ER2, Leica Biosystems) at pH 9 for 30 minutes at 95°C. The sections were stained with anti-EBNA2 (NBP2-50382, NOVUS), at 1:150 dilution, followed by incubation with the secondary antibody using the Bond Polymer Refine Red Detection (Leica Microsystems, Newcastle, United Kingdom), a polymeric AP-linker antibody conjugate system containing Fast Red solution as substrate chromogen.

For ICOSL, after antigen retrieval with Cell conditioner 1 (CC1, Ventana) at pH 6, for 20 min at 95°C, FFPE sections were incubated with anti-ICOSL antibody (CD274) (PA5-96572, Invitrogen) at 1:120 dilution for 40 minutes followed by incubation with a cocktail of enzyme-labeled secondary antibodies (HQ Universal linker and Multimer, Ventana). This complex was visualized with hydrogen peroxidase substrate and DAB chromogen, which produce a brown precipitate. Slides were then counterstained with Hematoxylin for 4 min and washed with reaction buffer. Finally, the slides were manually dehydrated through an ethanol series ($2 \times 80\%$ ethanol, 1 min each, $2 \times 90\%$ ethanol, 1 min each, $3 \times 100\%$ ethanol, 1 min each, $3 \times$ xylene, 1 min each), at room temperature, and mounted in Cytoseal xyl

(ThermoFisher Scientific, Waltham, MA). In parallel, tissue sections from the same cases without antibodies were used as a negative control.

RNA extraction from FFPE sections

Five sections (10 μ m) were obtained from FFPE tissues using fresh blades for each sample. The microtome was cleaned with absolute ethanol after each tissue block. Sections were collected in 1.5 ml tubes and deparaffinized twice with 1 ml xylene, pellets were washed with ethanol and incubated with Lysis Buffer (SV Total RNA isolation system - Promega) following the manufacturer's instructions. The concentration and quality of the RNA was evaluated using a NanoDrop ND-1000 Spectro-photometer (Thermo Fisher Scientific, Inc. USA).

Pre-miR-24 expression by RT-qPCR in U2932 EBNA2 and BJABK3

Precursor of miR-24, and U6 transcripts were detected using predesigned miScript Primer Assay primers purchased from QIAGEN. q-PCR assays, was used miScript SYBR Green PCR Kit (QIAGEN). All the q-PCRs were performed in an Applied Biosystems\StepOne Software v2.2.2 QPCR machine. The fold change of each transcript was calculated by the $2^{-\Delta\Delta C_t}$ formula.

Statistical analysis

Prism 9 software was employed for the data analysis. Measurement data that followed a normal distribution were expressed using mean and standard deviation. In comparing more than two groups, one-way ANOVA, Tukey's and Dunnett's test were employed, while two-tailed unpaired t test was used for comparing two groups. A statistically significant difference was only considered when the P-value was less than 0.05.

Supplementary figure legends

S Figure 1: Densitometry analysis of immunoblots

A: represents blots in Figure 1A; **B:** represents blots in Figure 2Ai and Bi; **C:** represents immunoblots in figure 6A. The statistical analysis was done using ordinary one-way ANOVA

Tukey's multiple comparisons test for S1A and S1C and by unpaired t test for S1B. P values indicate the significance of the mean with SD for each sample from three densitometry analyses.

S Figure 2: Decrease of pre-miR-24 in U2932 and BJABK3 expressing EBNA2

RT-qPCR quantification of the precursor-miR-24 (pre-miR-24) levels in

Ai: U2932 EBNA2 vs U2932 MPA vec, and

ii: in estradiol induced EBNA2 expressing BJABK3 vs its uninduced parental BJABK3. The housekeeping RNU6 was used to normalize the levels of pre-miR-24 in each sample. The P values were calculated through two-tailed unpaired t test. * $p < 0.05$, **** $p < 0.0001$.

S Figure 3: Inhibition of miR-24 decreases BCL-2 expression in U2932 EBNA2 transfected cells

Immunoblotting analysis of BCL2 in U2932 EBNA2 transfected with cntr inhibitor and anti-miR-24. β -actin was used as a loading control. Densitometry analysis shows relative quantification of decrease in BCL-2 expression normalized to β -actin expression from three independent experiments. Two-tailed unpaired t test was applied to estimate the p value. ** $p < 0.01$.

S Figure 4: Cumulative incidence of DLBCL cases diagnosed at our centers between 2018-2023.

S Figure 5: ICOSL expression in EBV negative GC (A and B) and non-GC (C and D) DLBCL biopsies by IHC

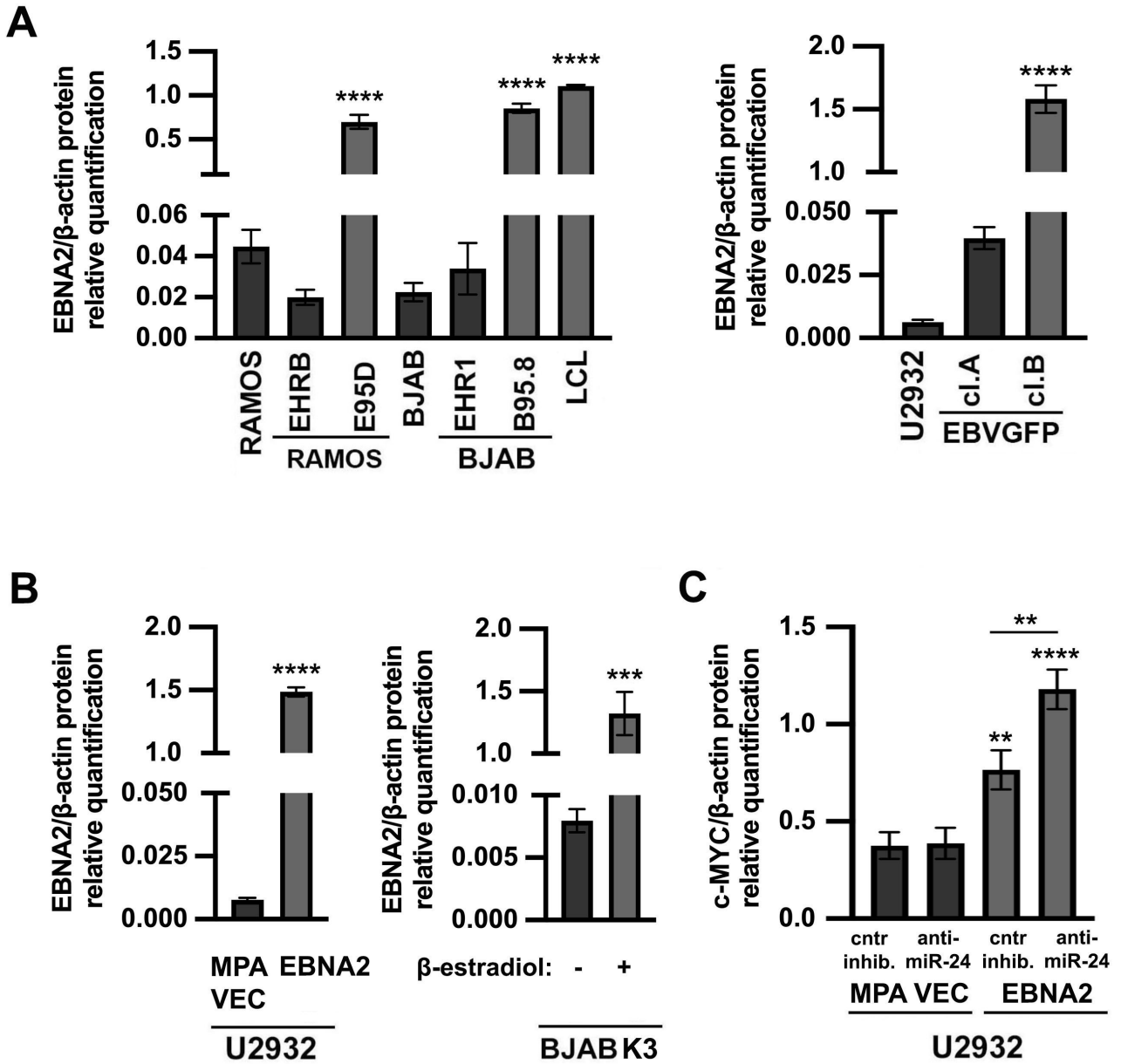
S Figure 6: EBNA2 and ICOSL expression in non-GC DLBCL biopsies

Expression of EBNA2 and ICOSL in five additional cases of EBV+/EBNA2+ non-GC biopsies is shown.

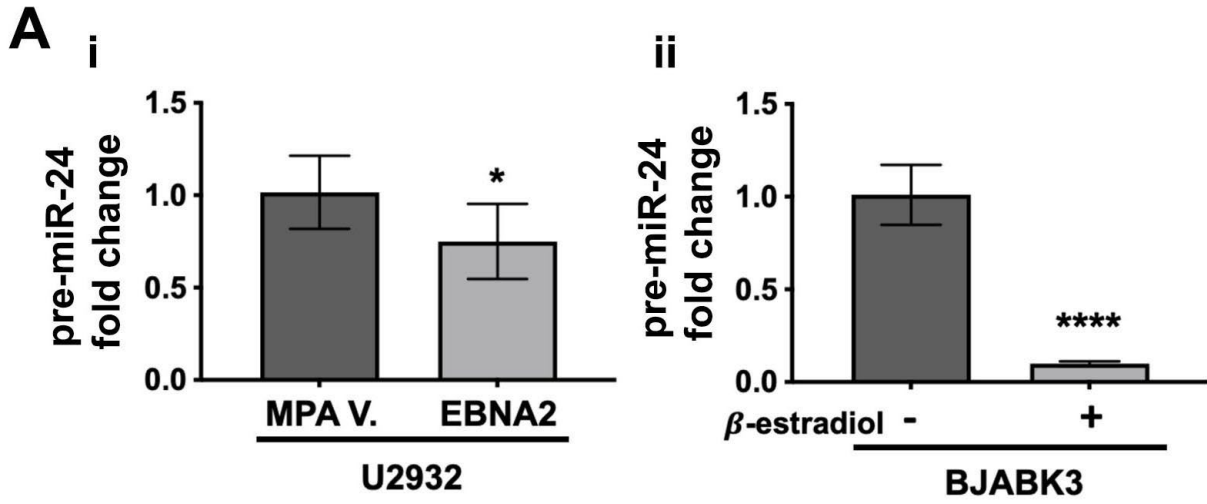
S Figure 7: ICOSL expression in reactive lymph node control

S Figure 8: ICOSL expression in lat II (LMP1+/EBNA2⁻) expressing DLBCL cases

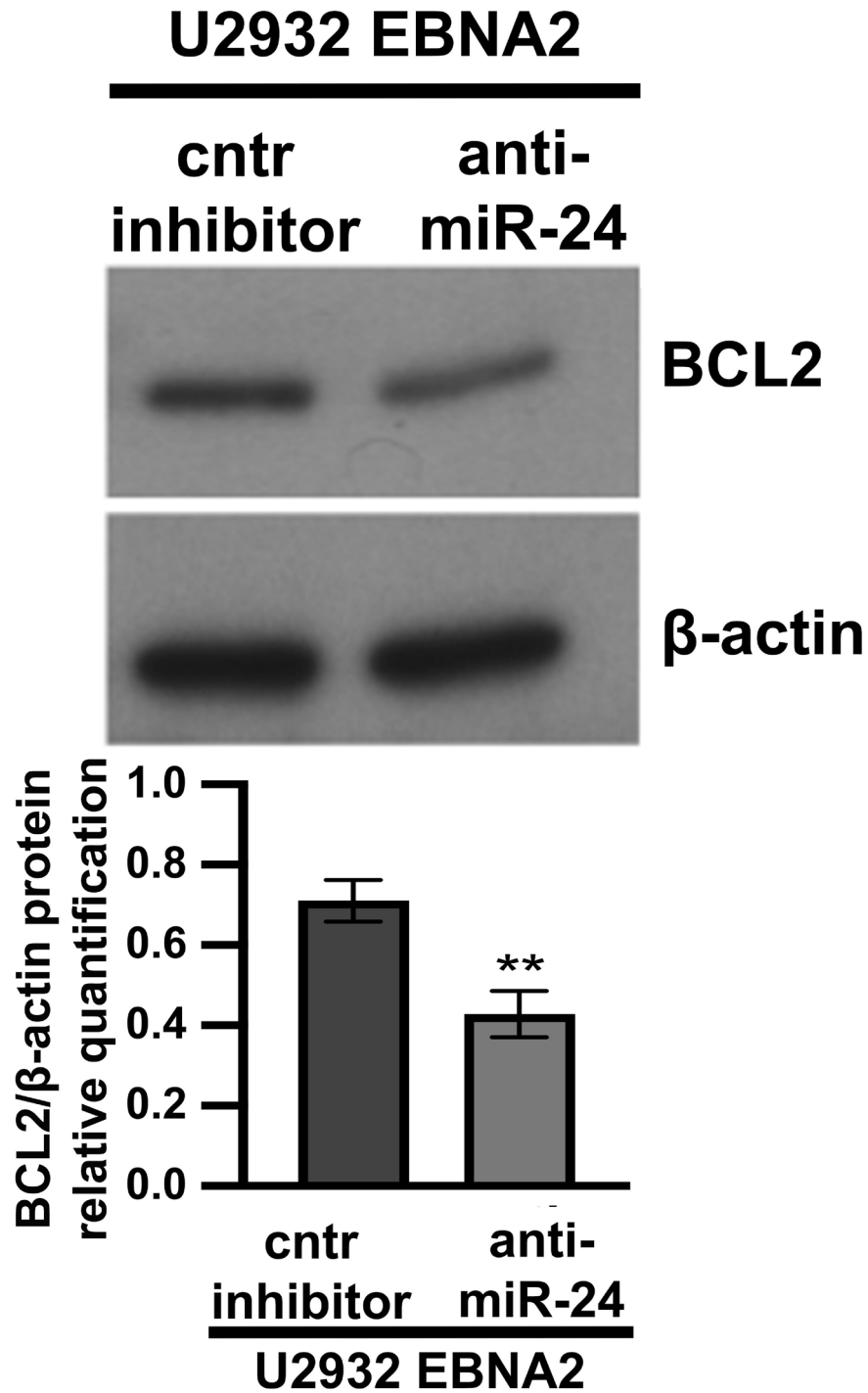
S Figure 9: ICOSL expression in cHL cases



Supplementary figure 1

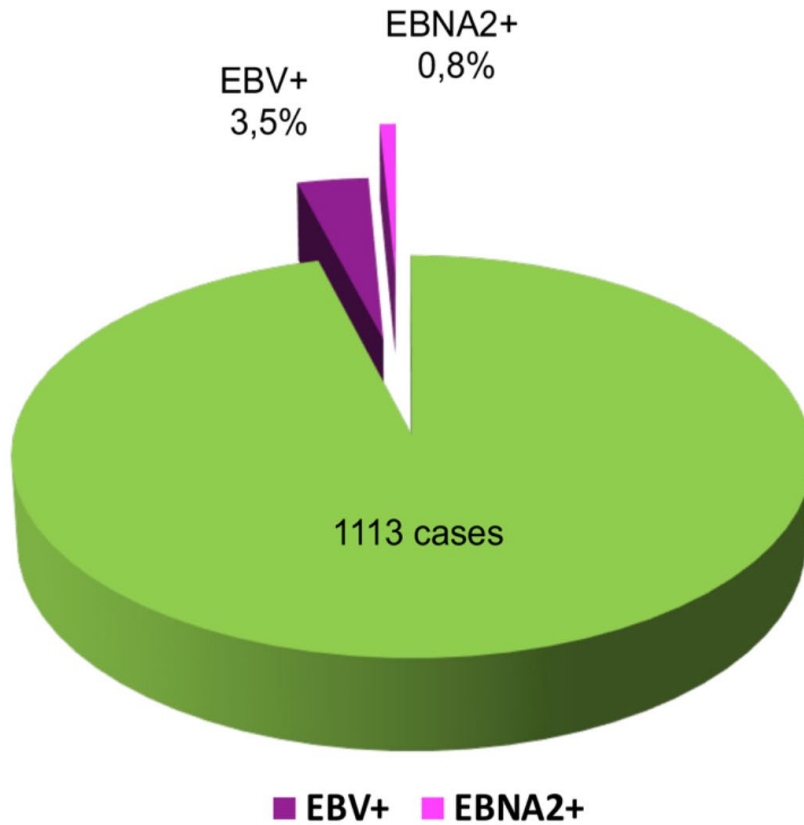


Supplementary figure 2



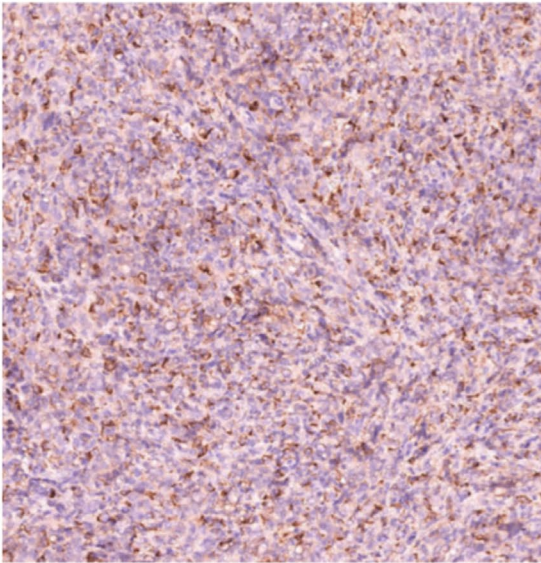
Supplementary figure 3

	Rome		Siena		Total
Cases	515	100%	598	100 %	1113
EBV+	18	3.5%	21	3.5%	39 (3.5%)
EBNA2+	5	1%	4	0.7%	9 (0.8%)

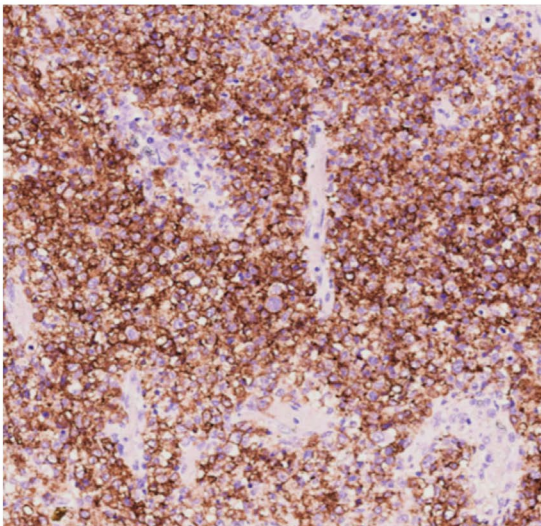
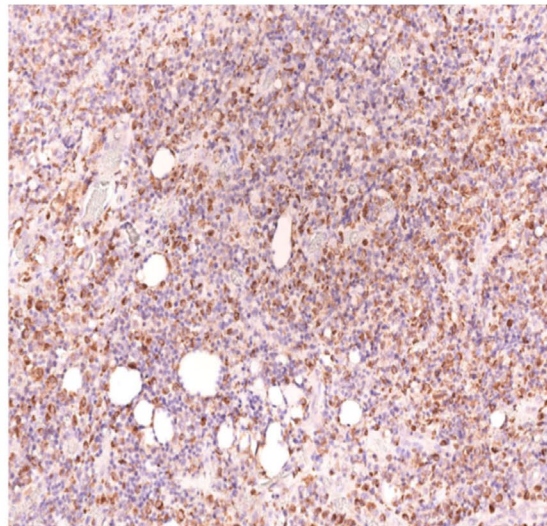


Supplementary figure 4

EBV neg GC DLBCL ICOSL

A**B**

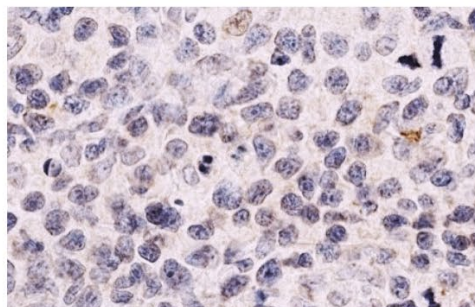
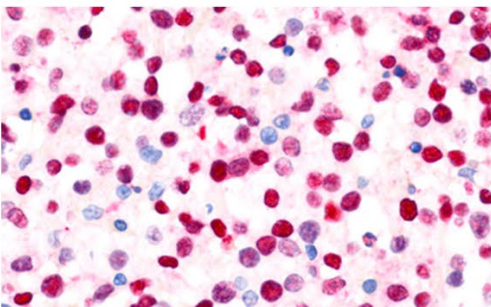
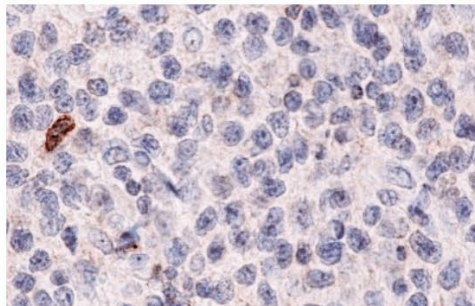
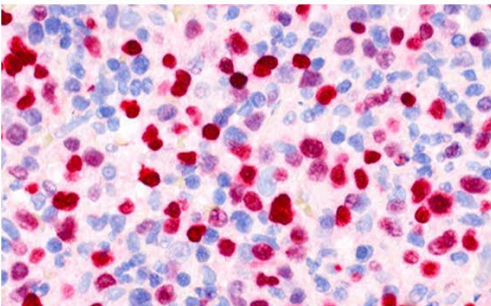
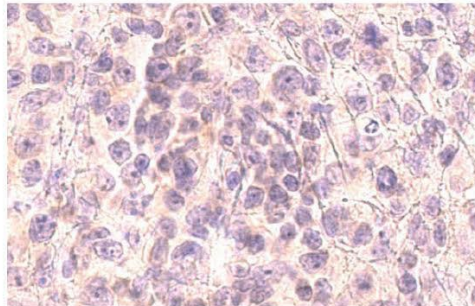
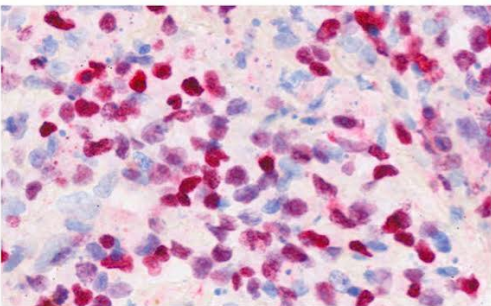
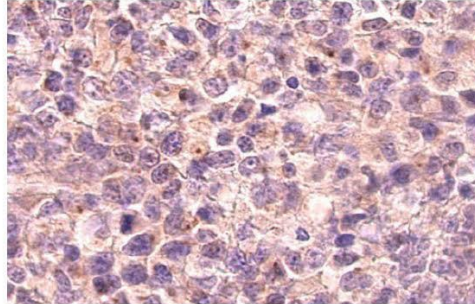
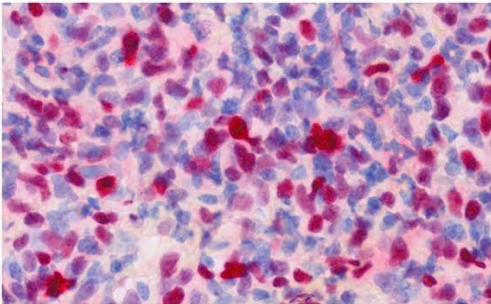
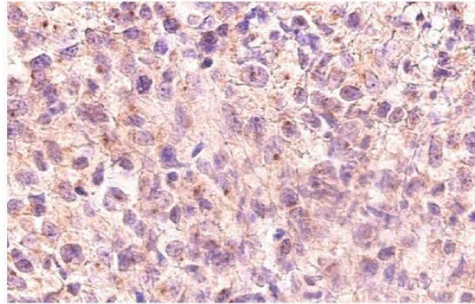
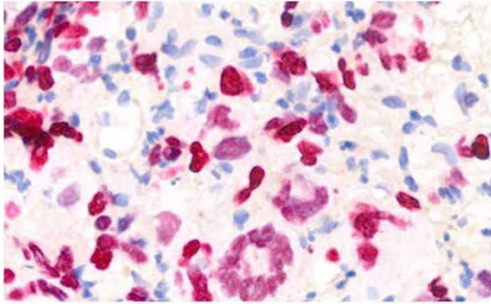
EBV neg non-GC DLBCL ICOSL

C**D**

Supplementary figure 5

EBNA2

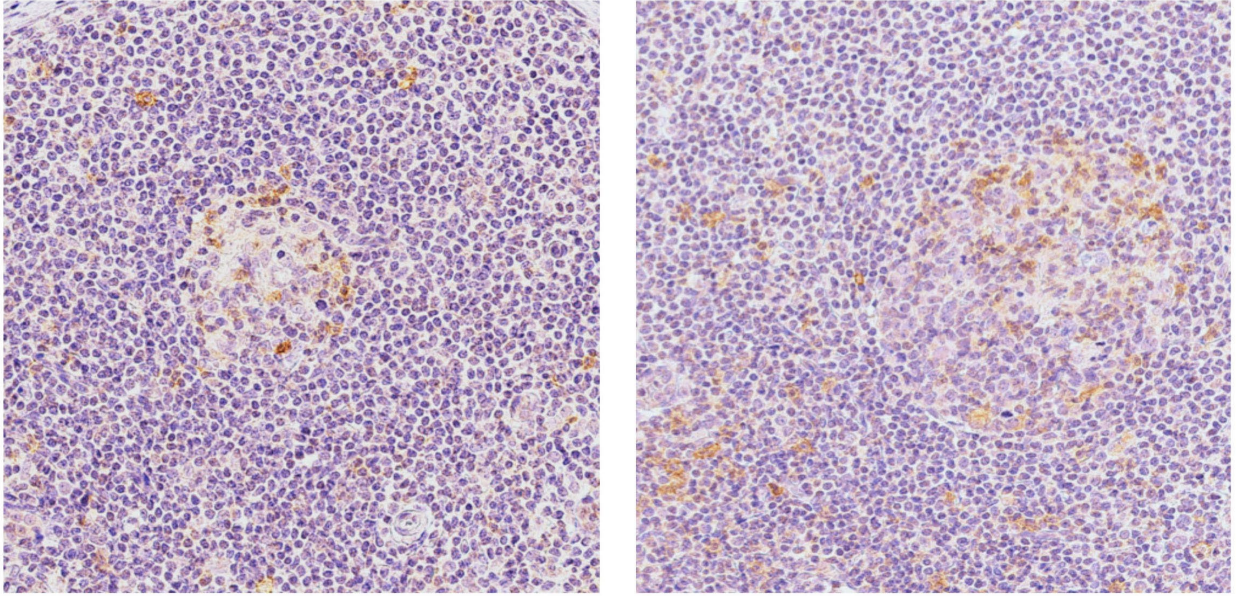
ICOSL



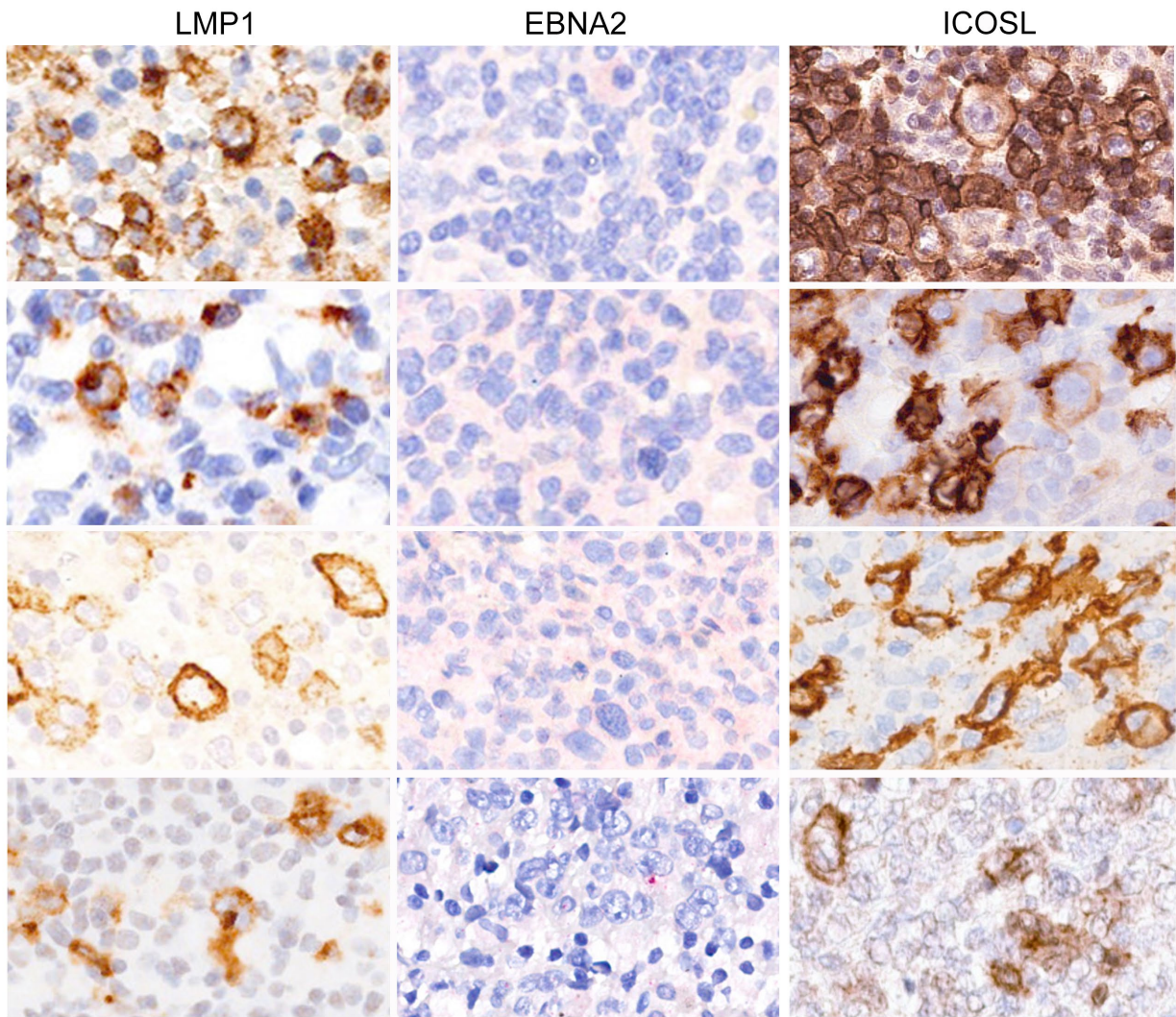
50 μ m

Supplementary Figure 6

ICOSL in reactive lymph node controls

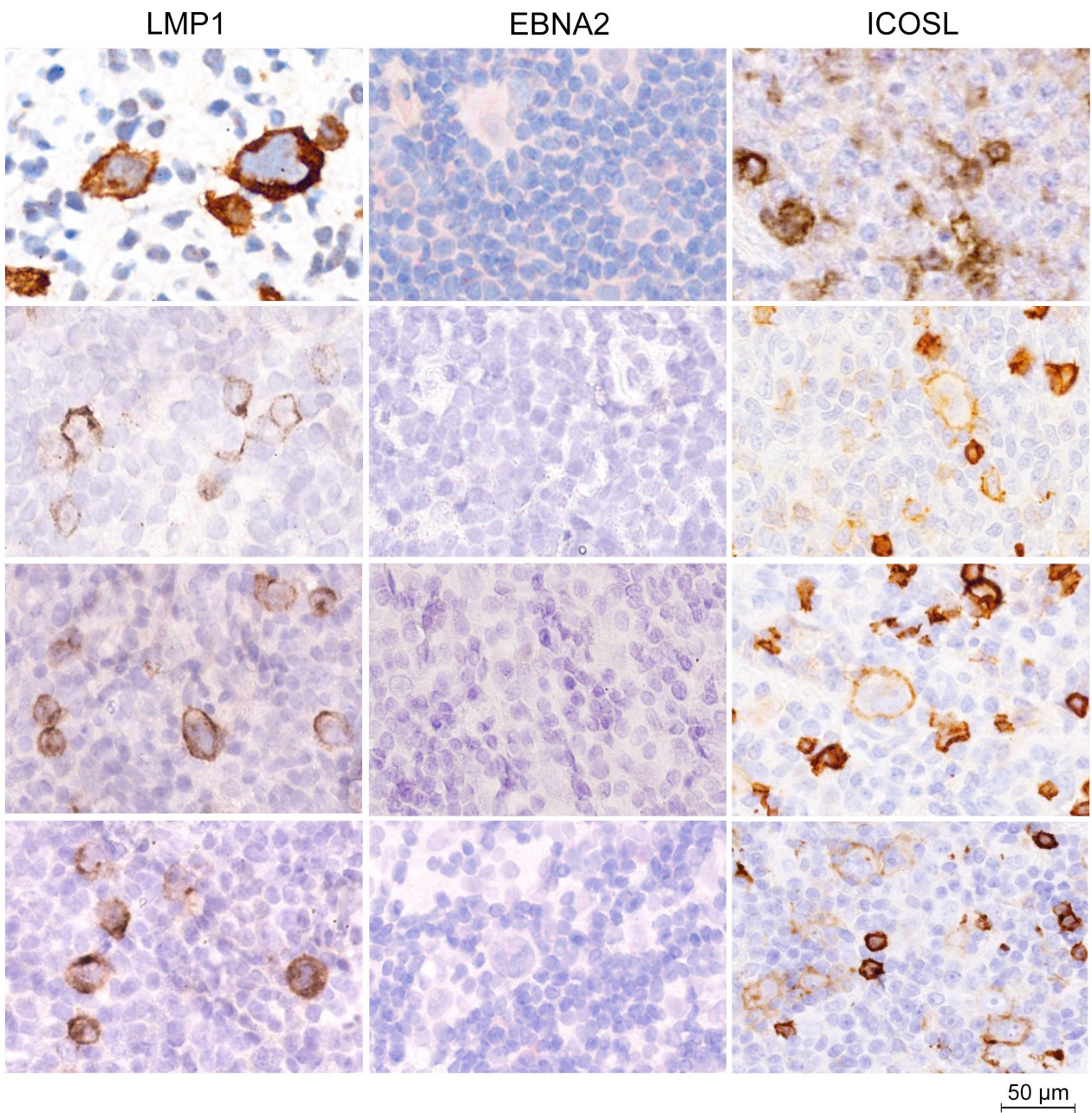


Supplementary figure 7



Lat II DLBCLs

Supplementary figure 8



HL

Supplementary figure 9

Supplementary Table 1: Cell lines used in this study

* B lymphoma cell lines used in this study. The B958 and P3HR1 are the two laboratory strains of

Cell line*	Tumor type and EBV status	EBNA2 status	Reference
U2932	EBV negative DLBCL	Negative	Amini et al ³⁹
U2932 EBVGFP Cl. A	In vitro infected	Negative	Boccellato et al ⁴⁰
U2932 EBVGFP Cl. B	In vitro infected	Positive	Boccellato et al ⁴⁰
U2932 EBNA2	Transfectants	Positive	Boccellato et al, ⁴⁰ Rosato et al, ²⁷ Anastasiadou et al ³⁸
Ramos	EBV negative BL	Negative	Ehlin Henriksson et al 1987 ⁴¹
Ramos E95D	In vitro infected with EBNA2 positive B958 strain	Positive	Ehlin Henriksson et al 1987 ⁴¹
Ramos EHRB	In vitro infected with strain lacking EBNA2	Negative	Ehlin Henriksson et al 1987 ⁴¹
Bjab	EBV neg, B cell lymphoma	Negative	Menezes et al, 1975 ⁴²
Bjab B958	In vitro infected with B958 strain	Positive	Wennborg et al ⁴³
Bjab EHR1	In vitro infected with strain lacking EBNA2	Negative	Wennborg et al ⁴³
BJABK3	B lymphoma	Inducible	Kempkes et al, 1995 ⁴⁴
P3HR1	BL	negative	Bornkamm et al 1982 ⁴⁵
Jijoye	BL	positive	Bornkamm et al 1982 ⁴⁵
EREB2-5	LCL	inducible	Kempkes et al, 1995 ⁴⁴

EBV with and without EBNA2 coding sequences respectively. EREB2-5 LCL contains estrogen inducible EBNA2.

Supplementary Table 2: Reagents used in this study

Reagent	Manufacturer	Working solution/dilution	Application
anti-EBNA2 Mouse monoclonal clone PE2, NBP2-50382	Novus Biologicals™, Biotechne	1:250/1:150	Western blot/IHC
Human anti-c-Myc Rabbit monoclonal antibody, D84C12	Cell Signaling Technology	1:250	Western blot
Human anti-Bcl-2 Rabbit monoclonal antibody, D55G8	Cell Signaling Technology	1:250	Western blot
Human anti-β-actin Mouse monoclonal, C4	Santa Cruz	1:5000	Western blot
Goat-anti-rabbit IgG Antibody, HRP conjugate	Advasta	1:10000	

Goat anti-Mouse IgG Antibody, HRP conjugate	Sigma-Aldrich, MERCK	1:10000	Western blot
ICOSL monoclonal Antibody (HK5.3), PE, eBioscience™	Thermo Fisher Scientific	1µL/sample	Flow cytometry
Rat IgG2a kappa Isotype Control (eBR2a), PE, eBioscience™	Thermo Fisher Scientific	1µL/sample	Flow cytometry
BD Pharmingen™ Purified Mouse Anti-Human CD28	BD Biosciences	1 µg/mL	T-cell activation
BD Pharmingen™ Purified Mouse Anti-Human CD3	BD Biosciences	1 µg/mL	T-cell activation
BD Pharmingen™ APC CD4 (L3T4), BD561840	BD Biosciences	1µL/sample	Flow cytometry
BD Pharmingen™ PACIFIC BLUE CD8, BD568207	BD Biosciences	1µL/sample	Flow cytometry
BD Pharmingen™ PE-CY7 IFN-γ, BD560924	BD Biosciences	1µL/sample	Flow cytometry
Cytofix/Cytoperm kit, BD555028	BD Biosciences	According to the instructions	Flow cytometry
Annexinv-PE, BD559763	BD Biosciences	According to the instructions	Flow cytometry
TaqMan® Assays: hsa-miR-24-3p Catalog number: 4427975, ID: 000402	Thermo Fisher Scientific Applied Biosystems™	1X	RT-qPCR/ ddPCR
TaqMan® Assays: RNU6 Catalog number: 4427975, ID: 001973	Thermo Fisher Scientific Applied Biosystems™	1X	RT-qPCR/ ddPCR
TaqMan™ Fast Advanced Master Mix for qPCR, no UNG, Catalog number: A44360	Thermo Fisher Scientific Applied Biosystems™	1X	RT-qPCR
ddPCR supermix for probe (no dUTP)	Bio-Rad Laboratories	1X	ddPCR
MISSION® Synthetic microRNA Inhibitor ath-miR416, Negative Control 1	Sigma-Aldrich, Merck	40nM	Transfection
MISSION® Synthetic microRNA Inhibitor, Human, hsa-miR-24-3p	Sigma-Aldrich, Merck	40nM	Transfection
DharmaFect Duo transfection reagent	GE Dharmacon	3µL/cell line	Transfection
MISSION 3'UTR Lenti GoClone of ICOSL and MISSION 3'UTR Lenti GoClone-Controls	Switchgear Genomics, Sigma-Aldrich, MERCK	10000 transducing units (TU)/cell line	Transduction
Polybrene	Sigma-Aldrich, Merck	8 µg/ml	Transduction
LightSwitch™ Assay Reagent (100 assays)	Switchgear Genomics, Sigma-Aldrich, Merck	100 µL/sample	Luciferase Assay Kit
ICOSL Polyclonal Antibody, PA5-96572	Invitrogen, Thermo Fisher Scientific	1:120	IHC
miScript II RT Kit HiFlex buffer	Qiagen	According to the instructions	RT
miScript Precursor Assay 100 reaction tubes, Pre-miR-24-3p and RNU6	Qiagen	1X	qPCR
Hs_ICOSLG_1_SG QuantiTect Primer Assay and Hs_GAPDH_1_SG QuantiTect Primer Assay predesigned primers	Qiagen	1X	qPCR
miScript SYBR Green PCR Kit	Qiagen	According to the instructions	qPCR

Supplementary Table 3: ICOSL expression in HL clinical samples

Case ID	Diagnosis* HL	Gender	Age	EBER	EBNA2	LMP1	ICOSL %
1	cHL	Male	44	+	-	+	>90@ (20)#
2	cHL	Female	67	+	-	+	70 (10)
3	cHL	Male	49	+	-	+	80 (30)
4	cHL mc	Male	39	+	-	+	40 (30)
5	cHL ns	Male	42	+	-	+	70 (10)
6	cHL ns	Male	47	+	-	+	30 (20)
7	cHL	Male	62	+	-	+	80 (20)
8	cHL	Female	28	+	-	+	40 (10)
9	cHL	Male	56	+	-	+	70 (20)
10	cHL	Male	57	+	-	+	30 (30)
11	cHL	Male	35	+	-	+	70 (10)

* MC-mixed cellularity, ns-nodular sclerosis, @ percentage positive RS cells, # () infiltrating cells